repressed chromatin state can be propagated in cis over short or long distances from initial sites of recruitment, to establish the global regulation of X chromosomes that is maintained throughout the lifetime of the animal.

References and Notes

1. B. J. Meyer, *Trends Genet.* **16**, 247 (2000).
2. V. H. Meller, M. I. Kuroda, *Adv. Genet.* **46**, 1 (2002).
3. K. Plath, S. Mlynarczyk-Evans, D. A. Nusinow, B. Panning, *Annu. Rev. Genet.* **36**, 233 (2002).
4. P. T. Chuang, D. G. Albertson, B. J. Meyer, *Cell* **79**, 459 (1994).
5. J. D. Lieb, E. E. Capowski, P. Meneely, B. J. Meyer, *Science* **274**, 1732 (1996).
6. J. D. Lieb, M. R. Albrecht, P. T. Chuang, B. J. Meyer, *Cell* **92**, 265 (1998).
7. K. A. Hagstrom, V. F. Holmes, N. R. Cozzarelli, B. J. Meyer, *Genes Dev.* **16**, 729 (2002).
8. H. E. Dawes *et al.*, *Science* **284**, 1800 (1999).
9. R. L. Kelley *et al.*, *Cell* **98**, 513 (1999).
10. Y. Park *et al.*, *Mol. Cell* **11**, 977 (2003).
11. V. H. Meller, B. P. Rattner, *EMBO J.* **21**, 1084 (2002).
12. Y. Park, R. L. Kelley, H. Oh, M. I. Kuroda, V. H. Meller, *Science* **298**, 1620 (2002).
13. H. Oh, Y. Park, M. I. Kuroda, *Genes Dev.* **17**, 1334 (2003).
14. E. M. Hedgecock, J. G. White, *Dev. Biol.* **107**, 128 (1985).
15. Materials and methods are available as supporting material on *Science* Online.
16. J. D. Lieb *et al.*, *Genetics* **156**, 1603 (2000).
17. G. Csankovszki, B. J. Meyer, unpublished observations.
18. B. J. Meyer, L. P. Casson, *Cell* **47**, 871 (1986).
19. C. C. Akerib, B. J. Meyer, *Genetics* **138**, 1105 (1994).
20. L. M. Miller, J. D. Plenefisch, L. P. Casson, B. J. Meyer, *Cell* **55**, 167 (1988).

21. We thank D. Albertson for X chromosome yeast artificial chromosomes; C. Y. Loh for cosmid array *yEx708* found to carry an X-recognition element; T. Cline, A. Severson, and C. Tsai for critical comments on the manuscript; and A. Lee, D. Akey, and T. Blumenthal for discussions. Some nematode strains were provided by the *Caenorhabditis* Genetics Center, funded by NIH's National Center for Research Resources. This work was supported by NIH Grant R37-GM30702 (B.J.M.) and NIH Fellowship F32-GM065007 (G.C.). B.J.M. is an investigator of the Howard Hughes Medical Institute.

Supporting Online Material

www.sciencemag.org/cgi/content/full/303/5661/1182/DC1
Materials and Methods
Fig. S1
References

24 October 2003; accepted 31 December 2003

An Engineered Pathway for the Formation of Protein Disulfide Bonds

Lluis Masip,[1] Jonathan L. Pan,[3,4] Suranjana Haldar,[5] James E. Penner-Hahn,[5] Matthew P. DeLisa,[1] George Georgiou,[1,2]* James C. A. Bardwell,[3,4]* Jean-François Collet[3]

We have engineered a pathway for the formation of disulfide bonds. By imposing evolutionary pressure, we isolated mutations that changed thioredoxin, which is a monomeric disulfide reductase, into a [2Fe-2S] bridged dimer capable of catalyzing O_2-dependent sulfhydryl oxidation in vitro. Expression of the mutant protein in *Escherichia coli* with oxidizing cytoplasm and secretion via the Tat pathway restored disulfide bond formation in strains that lacked the complete periplasmic oxidative machinery (DsbA and DsbB). The evolution of [2Fe-2S] thioredoxin illustrates how mutations within an existing scaffold can add a cofactor and markedly change protein function.

The pathways for the formation of disulfide bonds in secreted proteins of eukaryotic cells and bacteria are mechanistically very similar: Electrons are transferred from the protein thiols to soluble catalysts of disulfide bond formation, then to membrane-associated enzymes, and finally to terminal electron acceptors such as oxygen (*1*, *2*). In *Escherichia coli*, catalysis of disulfide bond formation is mediated by the periplasmic protein DsbA. DsbA is recycled by the membrane enzyme DsbB with concomitant reduction of quinones (*2*) (Fig. 1A). Inactivation of either the *dsbA* or the *dsbB* gene abolishes the oxidation of secreted proteins.

We sought to design a pathway for the formation of disulfide bonds that would be independent of the action of this disulfide catalytic machinery. Our aim was to create a pathway consisting of a protein carrier that acquires a disulfide bond within the cytoplasm, is subsequently translocated across the membrane, and then donates its disulfide bond stoichiometrically to periplasmic proteins, enabling their proper folding. Thus, a single protein would substitute for the entire DsbA-DsbB catalytic system, including its connection to the electron transport chain.

The designed pathway hinges upon three steps: (i) the selection of an appropriate protein that can form disulfide bonds, (ii) a means for forming a disulfide bond in the carrier protein within the normally reducing cytoplasm, and (iii) a mechanism for the export of the protein carrier, including its disulfide, across the membrane. Inactivation of the cytoplasmic redox balancing systems by deletion of the thioredoxin reductase (*trxB*) and glutathione reductase (*gor*) genes allows the formation of disulfide bonds in the cytoplasm (*3*). For the membrane translocation of a protein containing a disulfide, we chose to employ the twin arginine transporter pathway (Tat). Tat is responsible for the membrane translocation of proteins that have acquired cofactors in the cytoplasm and also for folded proteins, including those that contain disulfides (*4*).

We elected to use thioredoxin as the disulfide exchange protein for the designed pathway. Many enzymes with disulfide oxidoreductase activity, including protein disulfide isomerase and DsbA, contain a thioredoxin fold (*1*, *2*). These enzymes contain the active-site CXXC motif, where the cysteines reversibly form a disulfide bond and can undergo rapid thiol-disulfide exchange reactions. Although thioredoxin is normally a reductant, it can serve as a catalyst of disulfide bond formation in the cytoplasm under oxidizing conditions and can also weakly substitute for DsbA when secreted via the Sec secretory pathway (*5*). This ability to serve as a general periplasmic oxidant is completely dependent on recycling by DsbB.

dsbB$^-$ strains are nonmotile because of the misfolding of the flagella component FlgI, which contains an essential disulfide (*6*). The engineering of a pathway capable of mediating disulfide bond formation in the absence of DsbB should lead to the restoration of cell motility. TrxA was fused to the prototypical Tat-specific leader peptide ssTorA of the *E. coli* trimethylamine N-oxide reductase (TorA) protein and then expressed in the *E. coli* strain DR473 *dsbB*::kan5. This strain has an oxidizing cytoplasm and also carries a deletion in *dsbB*, so that disulfide bond formation in the periplasm is abolished. However, *E. coli* DR473 *dsbB*::kan5 expressing ssTorA-TrxA were nonmotile, indicating that this fusion is unable to mediate the formation of the critical disulfide bond in FlgI.

The central XX residues of the CXXC motif in proteins with a thioredoxin fold are critical for determining their redox properties (*7*). Specifically, substitution of the active-site CGPC dipeptide in thioredoxin by the sequence CPHC found in DsbA generates a thioredoxin mutant with a considerably more oxidizing redox potential (*7*). This mutation was generated, but the ssTorA-TrxA(CPHC) fusion also failed to restore motility, suggest-

[1]Department of Chemical Engineering and Institute for Cell and Molecular Biology, [2]Department of Biomedical Engineering, University of Texas, Austin, TX 78712, USA. [3]Department of Molecular, Cellular, and Developmental Biology, [4]Program in Cellular and Molecular Biology, [5]Department of Chemistry, University of Michigan, Ann Arbor, MI 48109, USA.

*To whom correspondence should be addressed. E-mail: gg@che.utexas.edu (G.G.); jbardwel@umich.edu (J.C.A.B.)

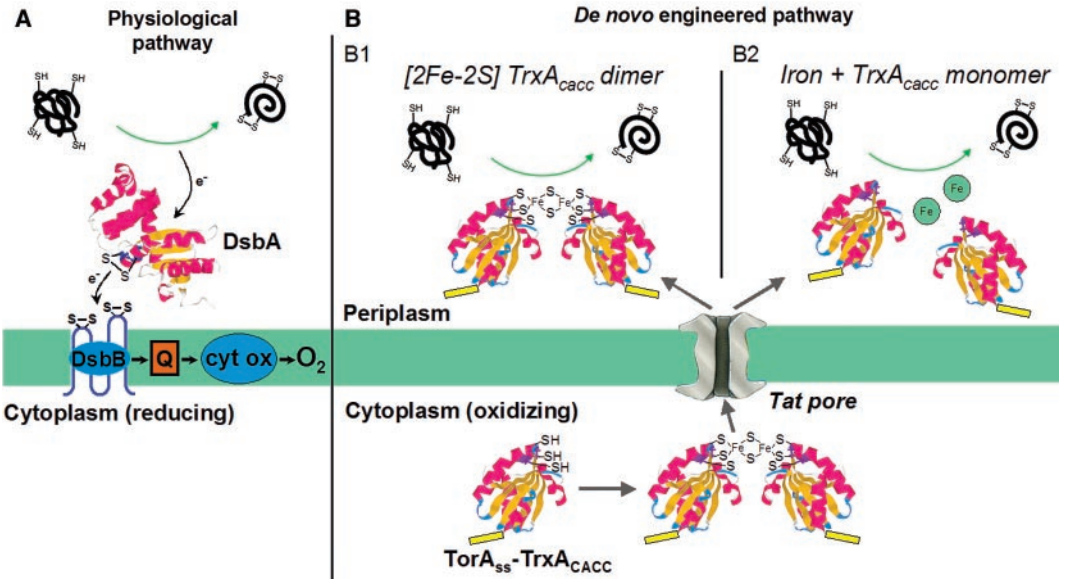

Fig. 1. Physiological and engineered disulfide bond formation pathways in the *E. coli* periplasm. (**A**) In the physiological pathway, DsbB provides oxidizing equivalents to DsbA, which acts as a general catalyst of protein thiol oxidation. e^-, electrons; Q, quinones; cyt ox, cytochrome oxidases. (**B**) Pathway for the formation of disulfide bonds by ssTorA-TrxA(CACC). Assembly of the [2Fe-2S] cluster occurs in strains with oxidizing cytoplasm (*trxB* or *trxB gor AhpC** mutants), and the dimeric form of the protein is subsequently exported through the Tat translocator. B1: Catalysis by dimeric TrxA(CACC) with the [2Fe-2S] center intact. B2: Catalysis by a two-part system in which the TrxA(CACC) dimer dissociates in the periplasm to release free iron and thioredoxin. Stoichiometric transfer of a disulfide from the cytoplasm may also be occurring (not shown).

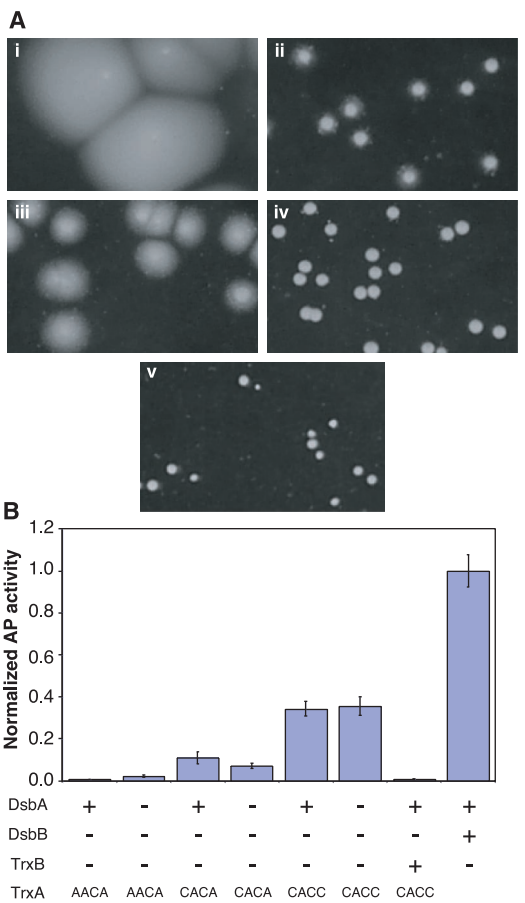

Fig. 2. In vivo disulfide bond formation. (**A**) Motility assay for the TrxA(CACC) mutant in different plasmid constructs and strain backgrounds. (*i*) *E. coli* DR473 (MC1000 *trxB gor ahpC**), our positive control; (*ii*) DR473 *dsbB*::kan5, our negative control; (*iii*) DR473 *dsbB*::kan5 containing the plasmid pTrc99a-ssTorA-TrxA(CACC); (*iv*) MC1000 *dsbB*::kan5 containing the plasmid pTrc99a-ssTorA-TrxA(CACC); (*v*) as in (*iii*) except that the RR dipeptide in ssTorA is substituted with KK to inhibit its export via the Tat pathway. Colonies were grown on motility plates for 40 hours at 37°C. (**B**) Alkaline phosphatase (AP) activity assay of TrxA(AACA), TrxA(CACA), and TrxA(CACC) in different strain backgrounds. *E. coli* MC1000 and derivatives with the corresponding pTrc99a-ssTorA-TrxA plasmid as shown were grown in Mops low-phosphate minimal media; the alkaline phosphatase activity in cell lysates was determined with p-nitrophenyl phosphate. Enzymatic activity was normalized on a per OD_{600} (optical density at 600 nm) basis and relative to the AP activity of MC1000 *trxB*. Error bars denote standard error.

ing that simply making the exported thioredoxin more oxidizing is insufficient to allow it to function independently of DsbB.

By imposing evolutionary pressure, we succeeded in isolating thioredoxin mutants in the absence of the recycling enzyme DsbB, which can confer motility in cells with an oxidizing cytoplasm (Fig. 2A). The sequence encoding the CXXC dipeptide in ssTorA-TrxA was randomized, the resulting library was expressed in DR473 *dsbB*::kan5, and colonies were screened for restoration of bacterial motility. A total of eight motile clones that encoded three different active-site sequences (CACC, CPCC, and CPSC) were isolated from ~4000 colonies screened. The three active-site mutants differed in their ability to restore motility [TrxA(CACC) ≈ TrxA(CPCC) > TrxA(CPSC)]. The ssTorA-TrxA(CACC) mutant that conferred greatest motility was examined in detail. Restoration of motility was dependent both on the presence of an oxidizing cytoplasm (Fig. 2A) and on export of the mutant protein via the Tat pathway. Substitution of the RR dipeptide within the ssTorA leader peptide with a KK sequence, a mutation that abolishes Tat export, rendered the cells nonmotile (Fig. 2A). Additionally, motility was impaired when the ssTorA leader peptide was substituted with the Sec-specific leader peptide from alkaline phosphatase (*8*).

Alkaline phosphatase is a periplasmic protein that contains two disulfides, both of which are required for its activity. The formation of active alkaline phosphatase was therefore used to evaluate whether other periplasmic proteins, in addition to FlgI, become oxidized by ssTorA-TrxA(CACC) in vivo (Fig. 2B). These experiments were carried out in *E. coli* strain MC1000 *trxB dsbB*::kan5 *dsbA*::cm, to determine whether the thioredoxin mutant could support protein oxidation in the absence of the complete DsbA-DsbB machinery. The designed pathway conferred ~40% of the alkaline phosphatase activity level observed in wild-type cells (Fig. 2B). Thus, ssTorA-TrxA(CACC) exported by the Tat pathway functions as a general periplasmic protein oxidant, independent of the DsbA-DsbB recycling machinery.

We investigated the mechanism of disulfide bond formation by ssTorA-TrxA(CACC) by individually substituting the N- and C-terminal Cys residues of the active site with alanine. Neither TrxA(AACC) nor TrxA(CACA)

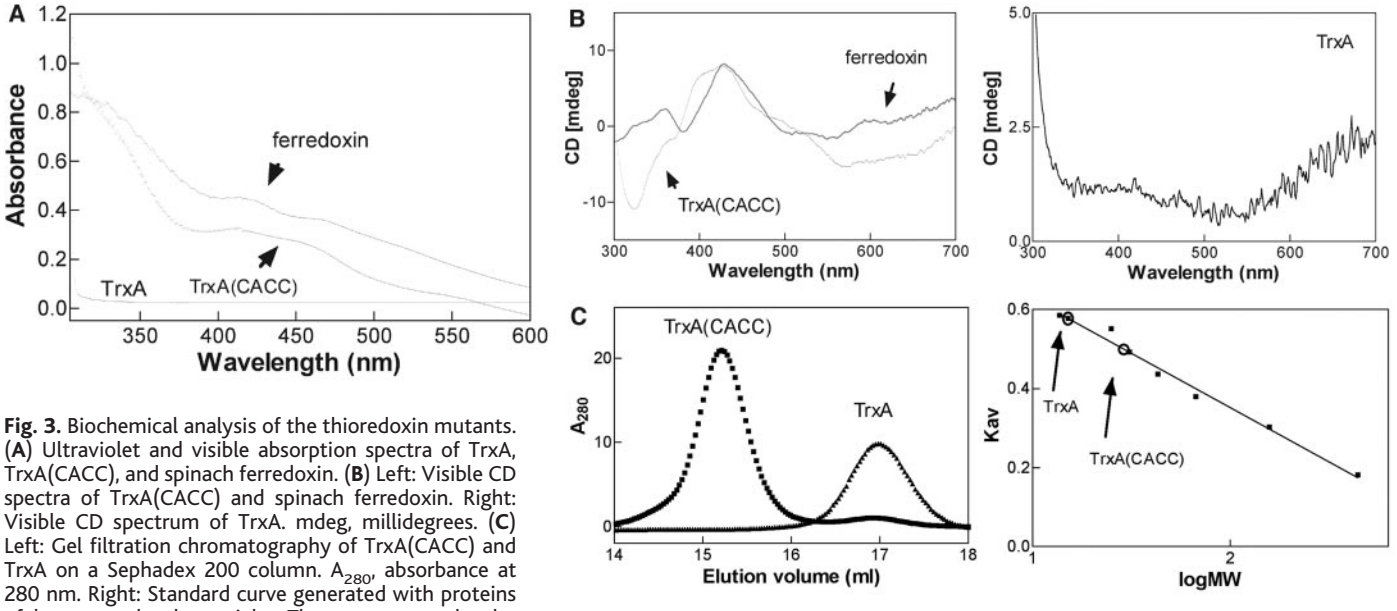

Fig. 3. Biochemical analysis of the thioredoxin mutants. (**A**) Ultraviolet and visible absorption spectra of TrxA, TrxA(CACC), and spinach ferredoxin. (**B**) Left: Visible CD spectra of TrxA(CACC) and spinach ferredoxin. Right: Visible CD spectrum of TrxA. mdeg, millidegrees. (**C**) Left: Gel filtration chromatography of TrxA(CACC) and TrxA on a Sephadex 200 column. A_{280}, absorbance at 280 nm. Right: Standard curve generated with proteins of known molecular weight. The apparent molecular weights of TrxA and TrxA(CACC) (open circles) were calculated according to this curve. K_{av}, partition coefficient. Squares represent the K_{av} of proteins of known molecular weights used to calculate the standard curve.

were capable of restoring motility in vivo. However, the latter mutant was capable of conferring ~25% of the alkaline phosphatase activity of TrxA(CACC) (Fig. 2B).

In order to biochemically characterize these proteins, the TrxA(CACC), TrxA(CACA), and TrxA(AACC) mutant proteins were overexpressed and purified to homogeneity. The purified TrxA(CACC) and TrxA(CACA) proteins were dark brown, in contrast to wild-type thioredoxin and TrxA(AACC), which were colorless. The absorbance spectrum of the TrxA(CACA) and TrxA(CACC) mutants showed peaks at 340, 412, and 452 nm and a shoulder at 560 nm, which is very similar to the iron-sulfur protein ferredoxin (Fig. 3A). The metal and sulfide content of these proteins was initially determined by Helmut Beinert (*9*) and subsequently by inductively coupled plasma atomic emission spectroscopy (ICP). TrxA(CACA) and TrxA(CACC) were found to contain one protein molar equivalent of iron and sulfide in a 1:1 stoichiometry, and no other metals were detected in significant levels. In contrast, the TrxA(AACC) mutant and the wild-type TrxA did not contain any significant amount of iron or sulfide or any other metals. Ultraviolet and visual spectroscopy revealed spectral characteristics of [2Fe-2S] clusters of the ferredoxin type (Fig. 3A). [4Fe-4S] clusters show very different spectral features, with characteristic absorption peaks at 325, 385, and 450 nm in the oxidized state (*10*) and a broad peak around 420 nm in the reduced state (*11*). Similarly, the circular dichroism (CD) spectroscopic characteristics of TrxA(CACC) were consistent with those of [2Fe-2S]–containing proteins, including spinach ferredoxin (Fig. 3B). TrxA(CACC) and TrxA(CACA) were both electron paramagnetic resonance (EPR) spectroscopy–silent at high or low temperatures, a feature that is typical of oxidized [2Fe-2S] clusters of the ferredoxin type (*10*). This type of cluster usually shows a strong EPR signal only on reduction, unless the cluster dissociates. However, on reduction of the mutant proteins with dithionite, the brown color disappeared and the protein remained EPR-silent, suggesting that the cluster had been destroyed. To unambiguously distinguish between different types of iron sulfur clusters, we performed extended x-ray absorption fine-structure spectroscopy (EXAFS) analysis on the two potentially iron sulfur–containing TrxA(CACC) and TrxA(CACA) mutant proteins. The results shown in Table 1 (particularly the coordination number) and in our supporting material are consistent with the presence of a [2Fe-2S] cluster of the ferredoxin type, but not with other iron sulfur clusters such as [4Fe-4S] clusters.

Table 1. Best-fit parameters for protein EXAFS data (lines 1 and 2) and crystallographic parameters for representative [2Fe-2S] (line 3) and [4Fe-4S] (line 4) clusters (*22*). R, absorber-scatterer distance; N, coordination number; σ^2, Debye-Waller factor.

Sample	Fe-S			Fe-Fe		
	R (Å)	N	$\sigma^2 \times 10^3$ (Å^2)	R (Å)	N	$\sigma^2 \times 10^3$ (Å^2)
CACC	2.27	4	9.2	2.73	1	5.1
CACA	2.28	4	10.1	2.76	1	7.0
$[Fe_2S_2(S_2\text{-o-xyl})_2]^{2-}$	2.26	4	—	2.70	1	—
$[Fe_4S_4(SPh)_4]^{2-}$	2.28	4	—	2.73	3	—

Four cysteine residues are often used to coordinate [2Fe-2S] clusters. Our mutants, however, contained a maximum of three cysteines in TrxA(CACC) and two cysteines in TrxA(CACA), raising the question of how they coordinate an iron sulfur cluster. During purification, the TrxA(CACC) and TrxA(CACA) mutants migrated as dimers in size exclusion chromatography (Fig. 3C). Incubation of the iron sulfur–containing TrxA(CACC) mutant at 55°C for 12 hours led to a loss of the brown color. The protein was shown to be iron-free, and gel filtration experiments indicated that the TrxA(CACC) protein was now monomeric. The fact that TrxA($C^{32}AC^{34}C$) is brown, iron sulfur–containing, and dimeric, whereas TrxA(AACC) is colorless, iron-free, and monomeric, strongly suggests that the iron sulfur cluster serves to dimerize thioredoxin and that the C^{32} and C^{34} residues, but not C^{35}, are involved in iron sulfur coordination. In fact, the iron sulfur cluster in the TrxA(CACA) mutant was more stable both during and after purification than the iron sulfur in the TrxA(CACC) mutant protein.

In addition to the variants of thioredoxin that contain three cysteines [TrxA(CACC) and TrxA(CPCC)], the motility screen also yielded TrxA(CPSC). Serine is chemically similar to cysteine and has also been ob-

served to coordinate iron sulfur clusters, mainly of the [2Fe-2S] type, though with reduced affinity (*12*). This might explain why this mutant protein showed the lowest activity in vivo. Although we have not studied the TrxA(CPSC) mutant [or the TrxA(CPCC) mutant] in detail, cells overexpressing the CPSC protein displayed a brown coloration, indicating that it likely contains an iron sulfur center.

We had sought to design a protein disulfide carrier that could be transferred from the cytoplasm into the periplasmic space. However, all three independent mutants that were selected for their ability to form disulfides in periplasmic proteins appear to incorporate a [2Fe-2S] cluster. This result provides genetic evidence that the iron sulfur cluster is required for the protein to mediate disulfide bond formation by TrxA. However, the [2Fe-2S] iron sulfur cluster alone is not sufficient for full thiol oxidation activity. C^{35} is also important for this function, because the ssTorA-TrxA(CACA) mutant contained a stable iron sulfur cluster yet conferred lower alkaline phosphatase activity and was not functional in the in vivo motility assay. Thus, optimal function of the engineered pathway requires both an iron sulfur cluster and a CXXC motif.

To determine if TrxA(CACC) could catalytically oxidize proteins, catalytic quantities of TrxA(CACC) or TrxA(CACA) were added to a 30-fold stoichiometric excess of reduced hirudin. Hirudin is a 65-residue protein, isolated from the medicinal leech, that has three essential disulfide bonds. In the presence of catalytic amounts of TrxA(CACC), reduced hirudin is converted to the native form (Fig. 4). This result demonstrates that the TrxA(CACC) protein is indeed capable of catalyzing oxidative protein folding in vitro. When EDTA was added to the reaction, only 15% of the reduced hirudin was oxidized to the native state (Fig. 4). Under anaerobic conditions, the yield of folded hirudin was similar to that obtained by EDTA treatment. Iron alone did not catalyze hirudin folding, even at concentrations as high as 0.3 mM, a 100-fold excess over TrxA(CACC) concentration. TrxA(CACA) used under identical conditions resulted in only 23% hirudin refolding, which was reduced to 2% in the presence of EDTA. Our results show that (i) TrxA(CACC) can catalyze the oxidation of hirudin, and it does so much more effectively than TrxA(CACA); (ii) in both cases, the reaction is metal dependent, because the yield and rate are much lower in the presence of EDTA (Fig. 4); and (iii) the catalyst is regenerated by oxygen, because hirudin is not folded efficiently when the reaction is performed anaerobically. It seems therefore that TrxA(CACC) is able to catalytically oxidize proteins in an oxygen and metal-dependent manner. In that regard, the evolved TrxA(CACC) enzyme resembles the iron-dependent sulfhydryl oxidase from bovine milk, which catalyzes the oxidation of sulfhydryls in proteins with O_2 as the electron acceptor (*13*). Although TrxA(CACC) is able to catalyze oxidative protein folding in vitro, we cannot rule out the possibility that in vivo stoichiometric transfer of disulfides may be partially responsible for its ability to substitute for the DsbA-DsbB pathway.

In general, iron sulfur clusters carry out one-electron redox reactions, whereas thiol-disulfide exchange reactions involve the transfer of two electrons. However, iron sulfur clusters have recently been shown to be involved in two-electron transfer reactions, including thiol-disulfide exchange. Notably, spinach ferredoxin:thioredoxin reductase was recently shown to catalyze the two-electron reduction of the active-site disulfide of thioredoxin f (*14*). Alternatively, in vivo the TrxA(CACC) mutant could be serving in vivo as the simultaneous exporter of iron and of a disulfide oxidoreductase (Fig. 1B). In this model, the incorporation of a [2Fe-2S] cluster into thioredoxin and the export of this two-component package could provide the periplasm with two catalysts, a redox active metal and a thiol-disulfide oxidoreductase that contains a CXXC active site. The breakdown of the [2Fe-2S] cluster after export of the TrxA(CACC) dimer should provide a significant concentration of free iron in the periplasm that could oxidize the TrxA(CACC) protein, in turn oxidizing substrate polypeptides. Metals are well known to be able to oxidize the cysteines in proteins in an air-mediated reaction, but this reaction is generally slow; furthermore, free metal concentrations in vivo are generally thought to be exceedingly low (*15*). On the other hand, thioredoxin is very rapidly oxidized by divalent metals and is capable of thiol-disulfide exchange reactions with rate constants ~10,000 times higher than those between proteins and dithiothreitol (*16*). To test this model, we examined the ability of wild-type TrxA to catalyze disulfide bond formation in the presence or absence of iron. In vitro, the folding of hirudin by TrxA in the presence of Fe^{2+} or Fe^{3+} was significantly less efficient compared to that obtained with an equimolar amount of TrxA(CACC) iron sulfur dimer. In vivo, export of TrxA via the Sec apparatus (by virtue of the alkaline phosphatase leader peptide) resulted in no alkaline phosphatase activity even when cells were incubated with a large excess of Fe^{2+} (*8*). While these results favor the model shown in Fig. 1B, panel 1, a contribution of dissociated TrxA(CACC) together with released iron (Fig. 1B, panel 2) to the formation of disulfide bonds in the periplasm certainly cannot be ruled out.

Independent of the precise mechanism, the iron sulfur cluster in thioredoxin is critical for the function of the designed pathway, either to control the reactivity of adjacent cysteines or as a means of transporting iron across the membrane. Iron sulfur clusters represent one of the most ancient of prosthetic groups, and one of the most ubiquitous, being found in more than 120 distinct classes of proteins, including components of the respiratory and photosynthetic electron transfer chains and a plethora of redox proteins involved in most areas of metabolism (*17*). The thioredoxin fold appears to represent a suitable scaffold for the incorporation of iron sulfur clusters. For example, a [2Fe-2S] cluster is naturally found in the thioredoxin-like ferredoxin from *Aquifex aeolicus* (*18*), and iron sulfur clusters have been inserted into thioredoxin by rational design (*19*), although these did not play a functional role. However, although the iron sulfur cluster is coordinated intramolecularly in the *Aquifex aeolicus* thioredoxin-like ferredoxin and in the rationally designed proteins, in the TrxA(CACC) and TrxA(CACA) mutants, the [2Fe-2S] cluster bridged two polypeptide chains.

Laboratory evolution has been employed extensively in studies that include alteration of the substrate specificity and stability of industrial enzymes, modulation of protein:protein

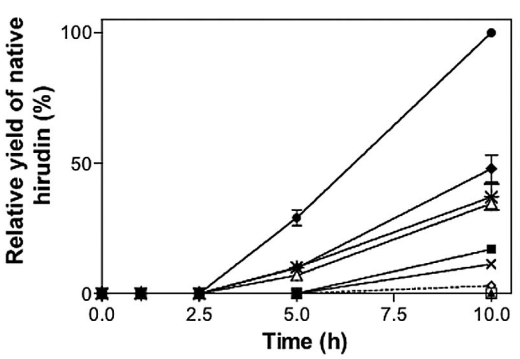

Fig. 4. Refolding of reduced hirudin by catalytic amounts of TrxA, TrxA(CACC), or TrxA(CACA). Reduced, denatured hirudin was incubated with catalytic amounts of TrxA(CACC) (solid circles), TrxA(CACA) (solid squares), or TrxA supplemented with stoichiometric amounts of Fe^{2+} (solid diamonds) or Fe^{3+} (asterisks). The effect of Fe^{2+} (solid triangles) and Fe^{3+} (open squares) alone or the addition of EDTA (1 mM) to TrxA (crosses), TrxA(CACC) (open triangles), or TrxA(CACA) (dashed line, open diamonds) was also determined. At different time points, aliquots were taken, the reaction was quenched by acidification, and samples were analyzed by high-performance liquid chromatography. The peak area corresponding to native hirudin was determined, and the relative amount of folded hirudin was calculated. The yield of native hirudin for the TrxA(CACC) mutant at the 10-hour time point was set as 100% (corresponding to between 70 and 95% conversion to native hirudin).

interactions and enzyme quaternary structure, and exploration of evolutionary relationships (*20*, *21*). We have, in essence, caught evolution in the act of adding an iron sulfur cluster to thioredoxin, enabling it to act as a thiol oxidant. Our results show that the acquisition of cofactors is evolutionarily a rather simple process, and our ability to generate an artificial pathway for oxidative protein folding highlights the plasticity of redox metabolism.

References and Notes

1. C. S. Sevier, C. A. Kaiser, *Nature Rev. Mol. Cell Biol.* **3**, 836 (2002).
2. J. F. Collet, J. C. A. Bardwell, *Mol. Microbiol.* **44**, 1 (2002).
3. P. H. Bessette, F. Aslund, J. Beckwith, G. Georgiou, *Proc. Natl. Acad. Sci. U.S.A.* **96**, 13703 (1999).
4. B. C. Berks, T. Palmer, F. Sargent, *Adv. Microb. Physiol.* **47**, 187 (2003).
5. L. Debarbieux, J. Beckwith, *Proc. Natl. Acad. Sci. U.S.A.* **95**, 10751 (1998).
6. F. E. Dailey, H. C. Berg, *Proc. Natl. Acad. Sci. U.S.A.* **90**, 1043 (1993).
7. E. Mossner, M. Huber-Wunderlich, R. Glockshuber, *Protein Sci.* **7**, 1233 (1998).
8. L. Masip *et al.*, unpublished data.
9. H. Beinert, *Anal. Biochem.* **131**, 373 (1983).
10. S. J. Lippard, J. M. Berg, *Principles of Bioinorganic Chemistry* (University Science Books, Mill Valley, CA, 1994), pp. 115–116.
11. B. A. Lazazzera, H. Beinert, N. Khoroshilova, M. C. Kennedy, P. J. Kiley, *J. Biol. Chem.* **271**, 2762 (1996).
12. J. M. Moulis, V. Davasse, M. P. Golinelli, J. Meyer, I. Quinkal, *J. Biol. Inorg. Chem.* **1**, 2 (1996).
13. V. G. Janolino, H. E. Swaisgood, *J. Biol. Chem.* **250**, 2532 (1975).
14. C. R. Staples *et al.*, *Biochemistry* **35**, 11425 (1996).
15. L. A. Finney, T. V. O'Halloran, *Science* **300**, 931 (2003).
16. A. Holmgren, *J. Biol. Chem.* **254**, 9113 (1979).
17. H. Beinert, R. H. Holm, E. Munck, *Science* **277**, 653 (1997).
18. J. Meyer, *FEBS Lett.* **509**, 1 (2001).
19. D. E. Benson, M. S. Wisz, W. Liu, H. W. Hellinga, *Biochemistry* **37**, 7070 (1998).
20. F. H. Arnold, *Nature* **409**, 253 (2001).
21. S. V. Taylor, P. Kast, D. Hilvert, *Angew. Chem. Int. Ed. Engl.* **40**, 3310 (2001).
22. J. M. Berg, R. H. Holm, *Metal Ions in Biology* **4**, 1 (1982).

23. We thank U. Jakob, P. Kiley, and H. Beinert for many helpful discussions; D. Ballou for help on spectrophotometric measurements; H. Beinert for doing the sulfide assays; T. Huston for performing the ICP–high resolution mass spectroscopy analyses; and T. Palmer and F. Sargent for reading the manuscript. X-ray absorption spectroscopy data were measured at the National Synchrotron Light Source, which is supported by the U.S. Department of Energy (contract no. DE-AC02-98CH10886), at line X9-B, which is supported by the NIH National Center for Research Resources (grant no. P41-RR01633). This work was supported by the Foundation for Research; NSF grant no. BES-220393 (G.G.); and NIH grant nos. GM-55090 (G.G.), GM-57039 and GM-64662 (J.C.A.B.), and GM-38047 (J.E.P.H.). J.F.C. is Charge de Recherches of the Belgian Fonds National de la Recherche Scientifique.

Supporting Online Material

www.sciencemag.org/cgi/content/full/303/5661/1185/DC1
Materials and Methods
SOM Text
Figs. S1 and S2
Table S1
References and Notes

15 October 2003; accepted 6 January 2004

The Structure of a Mycobacterial Outer-Membrane Channel

Michael Faller,[1] Michael Niederweis,[2] Georg E. Schulz[1]*

Mycobacteria have low-permeability outer membranes that render them resistant to most antibiotics. Hydrophilic nutrients can enter by way of transmembrane-channel proteins called porins. An x-ray analysis of the main porin from *Mycobacterium smegmatis*, MspA, revealed a homooctameric goblet-like conformation with a single central channel. This is the first structure of a mycobacterial outer-membrane protein. No structure-related protein was found in the Protein Data Bank. MspA contains two consecutive β barrels with nonpolar outer surfaces that form a ribbon around the porin, which is too narrow to fit the thickness of the mycobacterial outer membrane in contemporary models.

Mycobacteria are of medical importance because members of this genus cause tuberculosis and leprosy (*1*). The treatment of infections is difficult because mycobacteria fortify themselves with a thick impermeable cell envelope (*2*–*6*). One-third (dry mass) of this envelope consists of mycolic acids, which are exceptionally long α-branched β-hydroxy fatty acids of up to 90 carbon atoms (*1*, *7*). The mycolic acids are covalently attached by means of arabinogalactan chains to the peptidoglycan cell wall and form the inner leaflet of an outer membrane (*2*–*5*, *8*). The outer leaflet of this membrane consists of smaller and extractable lipids (*9*). The presence of an outer membrane was corroborated by an x-ray diffraction study showing a quasi-crystalline packing of lipids in the cell walls (*10*) and by freeze fracturing (*3*, *11*). The outer membrane shows low fluidity with phase-transition temperatures as high as 70°C (*12*) and is an extremely efficient permeation barrier protecting the cell from toxic compounds. Based on the lengths of the mycolic acids and their packing properties, as well as on electron micrographs of stained thin sections of mycobacterial cells, present models assume a nonpolar layer thickness of about 90 Å (*3*, *11*). The presence of an outer membrane seems to contradict the assignment of the mycobacteria to the Gram-positive branch based on 16*S* ribosomal RNA sequence comparisons (*13*). However, this inconsistency was recently reconciled by a whole-genome comparison that placed them equidistant to Gram-positive and -negative bacteria (*14*).

For the uptake of small hydrophilic nutrients, mycobacteria have special channels crossing their outer membrane, usually called porins. The porin concentration is low (*15*), which is likely to reduce the vulnerability and the growth rate. These porins were first detected in a cell wall extract of *Mycobacterium chelonae* with the use of lipid bilayer experiments (*16*). It showed a conductance of about 4 nS in 1 M KCl solutions. A similar porin was observed in extracts of *M. smegmatis* cells (*17*) and later purified, characterized, and named MspA (*18*). MspA is the major *M. smegmatis* porin; *M. smegmatis* also contains three other porins designated MspB, MspC, and MspD, which differ from MspA in only 2, 4, and 18 positions, respectively (*19*). No significant sequence similarity between the MspA group and any other protein was detected. The general cylindrical shape of MspA was established by electron microscopy (*15*). Here, we report the atomic structure of this porin, which shows a β structure that differs completely from its counterparts in Gram-negative bacteria (*20*, *21*) and constitutes the first structure of a mycobacterial outer-membrane protein.

For the expression in *Escherichia coli*, we used a designed *E. coli*–adapted gene of MspA without the signal peptide that is known to form an inactive 20-kD monomer and a channel-containing oligomer (*22*). The expression yielded appreciable amounts of monomeric MspA in the cytosol, which was purified by anion exchange chromatography and ammonium sulfate precipitation (*23*). After adding detergent and incubating overnight at a high concentration in the precipitate, monomeric MspA converted to oligomers with a high yield. The oligomers showed a mass greater than 100 kD in SDS–polyacrylamide gel electrophoresis. They formed crystals that were internally disordered and thus useless. Therefore, we produced about a dozen point mutants at predicted surface positions or exchange positions of the isomers MspB, MspC, and MspD (*23*). Among these mutants, $Ala^{96} \rightarrow Arg^{96}$ (A96R) (*24*) formed suitable crystals from fractions at the rise of the oligomer peak in a size exclusion chromatography (fig. S1). These fractions constituted merely 0.5% of the total MspA (*23*). Mutant A96R was

[1]Institut für Organische Chemie und Biochemie, Albert-Ludwigs-Universität, Albertstrasse 21, 79104 Freiburg im Breisgau, Germany. [2]Lehrstuhl für Mikrobiologie, Friedrich-Alexander-Universität Erlangen-Nürnberg, Staudtstrasse 5, 91058 Erlangen, Germany.

*To whom correspondence should be addressed. E-mail: schulz@bio.chemie.uni-freiburg.de